JOURNAL OF BACTERIOLOGY, Jan. 2011, p. 460–472 Vol. 193, No. 2
0021-9193/11/$12.00 doi:10.1128/JB.01010-10

argC Orthologs from *Rhizobiales* Show Diverse Profiles of Transcriptional Efficiency and Functionality in *Sinorhizobium meliloti*▽†

Rafael Díaz, Carmen Vargas-Lagunas, Miguel Angel Villalobos,‡ Humberto Peralta, Yolanda Mora, Sergio Encarnación, Lourdes Girard, and Jaime Mora*

Programa de Genómica Funcional de Procariotes, Centro de Ciencias Genómicas, Universidad Nacional Autónoma de México, Av. Universidad, Cuernavaca, Morelos C.P. 62210, Mexico

Received 24 August 2010/Accepted 31 October 2010

Several factors can influence ortholog replacement between closely related species. We evaluated the transcriptional expression and metabolic performance of ortholog substitution complementing a *Sinorhizobium meliloti argC* mutant with *argC* from *Rhizobiales* (*Agrobacterium tumefaciens*, *Rhizobium etli*, and *Mesorhizobium loti*). The *argC* gene is necessary for the synthesis of arginine, an amino acid that is central to protein and cellular metabolism. Strains were obtained carrying plasmids with *argC* orthologs expressed under the *speB* and *argC* (*S. meliloti*) and *lac* (*Escherichia coli*) promoters. Complementation analysis was assessed by growth, transcriptional activity, enzymatic activity, mRNA levels, specific detection of ArgC proteomic protein, and translational efficiency. The *argC* orthologs performed differently in each complementation, reflecting the diverse factors influencing gene expression and the ability of the ortholog product to function in a foreign metabolic background. Optimal complementation was directly related to sequence similarity with *S. meliloti*, and was inversely related to species signature, with *M. loti argC* showing the poorest performance, followed by *R. etli* and *A. tumefaciens*. Different copy numbers of genes and amounts of mRNA and protein were produced, even with genes transcribed from the same promoter, indicating that coding sequences play a role in the transcription and translation processes. These results provide relevant information for further genomic analyses and suggest that orthologous gene substitutions between closely related species are not completely functionally equivalent.

Synteny, gene neighboring, or conservation of chromosomal gene order has been proposed to be a result of the interdependence between a gene product and its genomic context. Conservation of a syntenic block could be favored by selective pressure because the arrangement allows the sequential or coordinated expression of genes that correctly integrate important metabolic functions (41, 64, 69). By a comparative analysis of four *Rhizobiales* species (namely, *Sinorhizobium meliloti*, *Agrobacterium tumefaciens*, *Mesorhizobium loti*, and *Brucella melitensis*), we found that syntenic genes exhibit striking differences compared to nonsyntenic genes, including increased operon and network organization, high sequence conservation, diminished evolutionary rates, essential functional role, and specific phylogenetic associations (32; H. Peralta, G. Guerrero, A. Aguilar, and J. Mora, unpublished data).

Orthologs encode similar functions sharing a common ancestor and exhibiting various degrees of conservation, due in large part to functional adaptation and cellular role in different species (45). We have proposed a new parameter termed "species signature" to extract the amount of amino acid residues specific for a given species, based on multiple sequence alignment. We hypothesized that the species signature represents the proportion of a particular sequence that responds to adaptation (32); it is a useful evolutive measure because we found a high direct correlation with the nonsynonymous substitution rate (Peralta et al., unpublished). Although orthologous genes of *Rhizobiales* encode proteins with high degrees of identity among several species, the proteins differ in many respects, including isoelectric point. Small differences in protein sequence may be the result of evolutionary adaptation in response to the particular intracellular environment of a given species. In this scenario, specific amino acid changes would be selected for optimal performance in a particular genetic background. Knight et al. (40) carried out a virtual analysis of proteomes of nearly 100 organisms and showed that there was a correlation between theoretical proteomes and ecological niches; conversely, there was no correlation between phylogeny and differences observed in the theoretical proteomes. Our previous work has shown that mutation of a single gene, *aniA* (a carbon flux regulator), produced a proteomic alteration of approximately 800 proteins (16, 22), indicating that the absence or modification of a single gene can result in complex changes in global gene expression. In this context, syntenic orthologs are ideal to evaluate the functional importance of species signature in related organisms.

The *Rhizobiales* order is a versatile group of bacteria that present very interesting features, such as a huge amount of genes, abundance of genes acquired by horizontal transfer events, a symbiotic or pathogenic association with higher organisms such as plants or animals, and the ability for nodulation and nitrogen fixation in some species (9, 13, 29, 31, 50, 54,

* Corresponding author. Mailing address: Programa de Genómica Funcional de Procariotes, Centro de Ciencias Genómicas-UNAM, Apdo. postal 565-A, Cuernavaca, Morelos C.P. 62220, México. Phone: 52 777 3114661. Fax: 52 777 3175094. E-mail: jmora@ccg.unam.mx.

† Supplemental material for this article may be found at http://jb.asm.org/.

‡ Present address: Centro de Investigación en Biotecnología Aplicada-IPN, Ex Hacienda San Juan Molino, Tlaxcala C.P. 90700, Mexico.

▽ Published ahead of print on 12 November 2010.

TABLE 1. Bacterial strains and plasmids used in this study

Strain or plasmid	Relevant characteristics[a]	Source or reference
Rhizobiales strains		
Sinorhizobium meliloti 1021^T	Wild type (type strain)	51
Rhizobium etli CFN42^T	Wild type (type strain)	62
Rhizobium etli CE3	Sm^r derivative of CFN42	53
Agrobacterium tumefaciens C58	Wild-type strain	ATCC 33970
Mesorhizobium loti MAFF303099	Wild-type strain	38
Sinorhizobium meliloti argC mutant	*S. meliloti* 1021 derivative, *argC*::ΩSp	This study
Escherichia coli strains		
DH5α	*supE44ΔlacU169*(ϕ80*lacZ*ΔM15) *hsdR17 recA1 endA1 gyrA96 thi-1 relA1*	34
HB101	*supE44 hsdS20* (r_B^- m_B^-) *recA13 ara-14 proA2 lacY1 galK2 rpsL20 xyl-5 mtl-1*	6
Plasmids		
pCR2.1 TOPO	Cloning vector for PCR products; Ap^r Km^r	Invitrogen
pJQ200SK$^+$	Suicide cloning vector; Gm^r	60
pBBR1MCS3	Broad host range cloning vector; Tc^r	42
pBBMCS53	Δp*lacZ* pBBR1MCS5 derivative, carrying the promoterless *gus* gene; Gm^r	28
pRK2073	Conjugation helper plasmid; Sm/Sp^r	4
pRK2013	Conjugation helper plasmid; Km^r	25
pHP45ΩSp	Plasmid containing the Ω-Sp interposon; Sp^r	57
pFGP1	pBBR1MCS3 derivative with *S. meliloti speB-argC* genes	This study
pFGP2	pBBR1MCS3 derivative with *A. tumefaciens speB-argC* genes	This study
pFGP3	pBBR1MCS3 derivative with *R. etli speB-argC* genes	This study
pFGP4	pBBR1MCS3 derivative with *M. loti speB-argC* genes	This study
pFGP5	pBBMCS53 derivative p*lac::gus* transcriptional fusion	This study
pFGP6	pBBMCS53 derivative p*argC*$_{Sm}$::*gus* transcriptional fusion	This study
pFGP7	pBBMCS53 derivative p*speB*$_{Sm}$::*gus* transcriptional fusion	This study
pFGP8	pBBMCS53 derivative p*lac-argC*$_{Sm}$::*gus* transcriptional fusion	This study
pFGP9	pBBMCS53 derivative p*lac-argC*$_{At}$::*gus* transcriptional fusion	This study
pFGP10	pBBMCS53 derivative p*lac-argC*$_{Re}$::*gus* transcriptional fusion	This study
pFGP11	pBBMCS53 derivative p*lac-argC*$_{Ml}$::*gus* transcriptional fusion	This study
pFGP12	pBBMCS53 derivative p*argC-argC*$_{Sm}$::*gus* transcriptional fusion	This study
pFGP13	pBBMCS53 derivative p*argC-argC*$_{At}$::*gus* transcriptional fusion	This study
pFGP14	pBBMCS53 derivative p*argC-argC*$_{Re}$::*gus* transcriptional fusion	This study
pFGP15	pBBMCS53 derivative p*argC-argC*$_{Ml}$::*gus* transcriptional fusion	This study
pFGP16	pBBMCS53 derivative p*speB-argC*$_{Sm}$::*gus* transcriptional fusion	This study
pFGP17	pBBMCS53 derivative p*speB-argC*$_{At}$::*gus* transcriptional fusion	This study
pFGP18	pBBMCS53 derivative p*speB-argC*$_{Re}$::*gus* transcriptional fusion	This study
pFGP19	pBBMCS53 derivative p*speB-argC*$_{Ml}$::*gus* transcriptional fusion	This study
pFGP20	pBBMCS53 derivative carrying the *S. meliloti argC* gene under its promoter	This study
pFGP21	pBBMCS53 derivative carrying the *A. tumefaciens argC* gene under the control of the *S. meliloti argC* promoter.	This study
pFGP22	pBBMCS53 derivative carrying the *R. etli argC* gene under the control of the *S. meliloti argC* promoter	This study
pFGP23	pBBMCS53 derivative carrying the *M. loti argC* gene under the control of the *S. meliloti argC* promoter	This study
pFGP24	pBBMCS53 derivative p*argC*$_{At}$::*gus* transcriptional fusion	This study
pFGP25	pBBMCS53 derivative p*argC*$_{Re}$::*gus* transcriptional fusion	This study
pFGP26	pBBMCS53 derivative p*argC*$_{Ml}$::*gus* transcriptional fusion	This study

[a] Tc^r, tetracycline resistance; Ap^r, ampicillin resistance; Sm^r, streptomycin; Sp^r, spectinomycin resistance; Km^r, kanamycin resistance; Gm^r, gentamicin resistance.

65). In addition to a circular chromosome, some rhizobia carry secondary chromosomes or plasmids of high molecular size. Arginine is an essential amino acid in bacteria, and its synthesis requires a great deal of energy and reducing power (14, 49, 63). Arginine is the most common nitrogen storage compound and precursor of polyamine synthesis (48, 61). *argC* genes are commonly organized in operons, exemplified by the *Escherichia coli argCBH* operon (56). In *R. etli*, the *argC* mutation affects growth capacity using ammonium as the sole nitrogen source and results in failure to nodulate the common bean root (23).

We were interested in exploring whether the species signature (particular amino acid sequence variations) in orthologous syntenic genes reflects adaptations to the particular conditions of a given species, both intracellular (interactions with other enzymes and metabolites) and extracellular. The effect of heterologous complementation of an *S. meliloti argC* mutant with the corresponding ortholog from other *Rhizobiales* species (*A. tumefaciens*, *R. etli*, and *M. loti*) was compared in terms of growth, excretion of organic compounds, transcriptional and enzymatic activity, and molecular parameters such as mRNA and translation efficiency. An analysis of the putative *speB-argC* operon was also carried out to define a novel functional *argC* promoter.

MATERIALS AND METHODS

Bacterial strains and growth conditions. Bacterial strains and plasmids used in the present study are listed in Table 1. The *S. meliloti argC* mutant was obtained

cloning an 1.3-kb *argC* SmaI-SpeI fragment into the pJQ200SK+ vector (60). The pHP45Ω-Sp plasmid (57) was digested with BamHI to obtain the Ω-Sp interposon, and it was cloned on a BglII site of the *argC* fragment. The obtained plasmid was conjugated to the *S. meliloti* 1021 wild-type strain, and double recombinants were selected on minimal medium (MM) (19) (1.2 mM K_2HPO_4, 0.8 mM $MgSO_4$, 1.5 mM $CaCl_2$, 0.01 mM $FeCl_3$), supplemented with 10 mM succinic acid and 10 mM ammonium chloride (NH_4Cl). The wild-type, *argC* mutant, and *argC* complemented strains were maintained in PY medium, as described previously (19). When necessary, antibiotics were added at the following concentrations: nalidixic acid, 20 μg/ml; streptomycin, 200 μg/ml; spectinomycin, 100 μg/ml; gentamicin, 15 μg/ml; and tetracycline, 5 μg/ml. MM was used supplemented with 10 mM succinic acid or mannose as a carbon source and 10 mM ammonium chloride (NH_4Cl) or potassium nitrate (KNO_3) as a nitrogen source. Cultures were grown aerobically at 30°C in a shaker at 200 rpm for all experiments. To confirm that the complementation phenotypes observed were due exclusively to plasmid-encoded sequences, in some cases the plasmids were cured and conjugation repeated. Similar results were obtained (data not shown).

Introduction of overlapping ends by PCR amplification using chimeric primers. Hybrid fusion genes containing *argC* genes from *S. meliloti* 1021, *A. tumefaciens* C58, *R. etli* CE3, and *M. loti* MAFF303099 under the control of different promoters were constructed by using overlap extension PCR methodology (66). Chimeric primers were designed with additional 5′ sequences to introduce homologous ends into the fragments to be fused. We used Oligo 6.0 software to construct the primer sequences, and the primers were purchased from the Unidad de Síntesis Química (IBt-UNAM).

The *S. meliloti argC* and *speB* regulatory regions containing overlapping ends corresponding to each *argC* ortholog were amplified by PCR using genomic DNA from *S. meliloti* strain 1021 as the template. Eight different PCRs were performed to obtain specific 896- and 500-bp PCR products with distinct overlapping ends. The specific primers used to generate the hybrid genes are listed in Table S1 in the supplemental material Amplification was carried out using a MasterCycler 5330 (Eppendorf, Hamburg, Germany) and AccuPrime *Pfx* DNA polymerase (Invitrogen). The reaction conditions were as follows: denaturation at 94°C for 2 min, followed by 30 cycles of 94°C for 20 s, 62°C for 30 s, and 68°C for 60 s. A final elongation step was carried out at 72°C for 10 min.

The complete *argC* coding regions of *A. tumefaciens* C58 (932 bp), *R. etli* CFN42 (932 bp), and *M. loti* MAFF303099 (926 bp) were obtained by PCR amplification using chimeric primers containing the *S. meliloti argC* promoter region overlapping ends. Total DNA from each strain was used as a template. The reaction conditions were as follows: denaturation at 94°C for 2 min, followed by 30 cycles of 94°C for 15 s and 68°C for 60 s. A final elongation step was carried out at 72°C for 10 min. For these reactions, Pfx50 DNA polymerase from Invitrogen was used. All PCR products were analyzed by agarose gel electrophoresis and then purified by using a QiaQuick gel extraction kit from Invitrogen.

To join the two DNA fragments, 1 μl of each PCR was mixed and cycled without primers. The reaction conditions were as follows: an initial denaturation step at 95°C for 2 min; followed by 20 cycles of 95°C for 1 min; annealing at 68°C for 10 s, 66°C for 5 s, 64°C for 5 s, and 62°C for 5 s; and extension at 72°C for 90 s. An additional extension was carried out at 72°C for 10 min. Portions (2 μl) of this reaction were mixed with the appropriate outer primers, and the assembled products were recovered. The reaction conditions were as follows: initial denaturation at 95°C for 2 min, followed by 30 cycles of 95°C for 15 s and 70°C for 2 min, followed by an additional extension at 72°C for 10 min. The reactions were carried out by using AccuPrime *Taq* DNA Polymerase High Fidelity (Invitrogen). The hybrid genes were cloned into pCR2.1 TOPO. All plasmids were sequenced to confirm that the fused gene was obtained with no nucleotide changes. Each set of constructs presented identical flanking sequences, including the regulatory ones, so that the only variant was the *argC* coding sequence from each organism.

Construction of plasmids for complementation experiments. Plasmids able to replicate in *S. meliloti* were constructed by using the cloning vector pBBMCS53, a derivative of pBBR1MCS5 carrying the promoterless *gus* gene (28). This permitted the complementation and the transcriptional monitoring with the same construction. The sequences of all primers used are listed in Table S1 in the supplemental material. A plasmid, pFGP20, containing a 1,889-bp PCR fragment corresponding to the *S. meliloti argC* regulatory and coding regions, was constructed. Total DNA isolated from *S. meliloti* strain 1021 was used as the template for PCR with the primers SmUpXba and Lw_H1_PSm. The resulting fragment was cloned into pCR2.1 TOPO for sequencing (pTOPO::p$argC_{Sm}$-$argC_{Sm}$). An 896-bp regulatory region and the complete *argC* coding region were cloned into the pBBMCS53 plasmid as a 1,937-bp XbaI fragment. The 1,906-bp EcoRI hybrid fragment from TOPO::p$argC_{Sm}$-$argC_{At}$ was cloned into pBBMCS53 to generate pFGP21. To generate pFGP22, the 1,924-bp XbaI-BamHI fragment from TOPO::p$argC_{Sm}$-$argC_{Re}$ was cloned into pBBMCS53. The XbaI-BamHI fragment from TOPO::p$argC_{Sm}$-$argC_{Ml}$ was cloned into the same vector to generate pFGP23. The resulting recombinant plasmids were analyzed by restriction enzyme digestion and nested PCR to confirm that they contained the proper hybrid gene. Another complete set of plasmids was obtained, containing only *argC* genes on pBBR1MCS3 vector, under each of the mentioned promoters in order to be used in mRNA and proteomic ArgC detection and quantification.

Construction of β-glucuronidase transcriptional fusions. To analyze the level of expression of each used promoter and *argC* orthologs or their segments, we constructed β-glucuronidase (*gus*) transcriptional gene fusions. The recombinant plasmids described above were used as templates for PCR with the primers SmUpXba and FusC_gus_R. Amplified fragments of the correct size were cloned into pCR2.1 TOPO. Four additional plasmids were constructed carrying the 896-bp regulatory region of *S. meliloti argC* and the complete *argC* gene sequence of each species (lacking the last 50 nucleotides) fused with the *gus* gene. This cassette was inserted into pBBMCS53 as an XbaI-KpnI fragment. Plasmids pFGP12, pFGP13, and pFGP14 contained an 1,828-bp XbaI-KpnI fragment that corresponded to *argC* genes from *S. meliloti*, *A. tumefaciens*, and *R. etli* under the *S. meliloti argC* promoter, respectively. A plasmid containing the *M. loti argC* gene under the control of the *S. meliloti argC* promoter was constructed by cloning an 1,822-bp XbaI-KpnI fragment in pBBMCS53 (pFGP15).

Conjugative transfer of plasmids from *E. coli* to *Rhizobium* was done by triparental mating, using either pRK2013 (25) or pRK2073 (4) as a helper. For determination of plasmid profiles, a modified Eckhardt procedure was used (36).

Determination of plasmid copy number. The plasmid copy number was assessed in p*speB* promoter-plasmids, by PCR, using *tetA* gene from plasmids and *rpoA*, a chromosomal gene, to calibrate the results. Complemented strains were grown for 8 h with shaking (200 rpm) at 30°C in MM containing succinate-ammonium. The initial inoculation was at an optical density at 540 nm (OD_{540}) of 0.05. An aliquot of the cell culture (2 ml) was removed, and the cells were washed with sterile, deionized water. The cells were lysed by heat treatment at 95°C for 20 min. The lysate was diluted 500-fold and used as a template for PCR amplification of the *tetA* gene (for quantification of plasmid) and *rpoA* gene (as an endogenous, single-copy control). Amplification and detection of DNA by real-time PCR was performed by using the ABI Prism 7300 sequence detection system (Applied Biosystems) in optical-grade 96-well plates. Triplicate samples were routinely used for the determination of DNA by real-time PCR. The reaction conditions for amplification of DNA were as follows: 50°C for 2 min and 95°C for 10 min, followed by 40 cycles of 95°C for 15 s and 60°C for 1 min. The data analysis was carried out by using sequence detection software (version 1.6.3; Applied Biosystems).

RACE. The transcriptional start site of the *S. meliloti argC* gene was identified by using the 5′ rapid amplification of cDNA ends (5′RACE) system (version 2.0; Invitrogen). cDNA was synthesized from 1 to 5 μg of total RNA with the complementary primer argCGSP-1 (corresponding to nucleotides 415 to 430 of the *argC* coding region). After first-strand cDNA synthesis, mRNA was removed by treatment with RNase and then the cDNA was purified by using a SNAP column (Invitrogen). Terminal deoxynucleotidyltransferase and dCTP were used to add homopolymeric tails to the 3′ ends of the cDNA. Nested PCR was carried out by using the gene-specific primer argCGSP-2 (corresponding to nucleotides 340 to 355) and the abridged anchor primer (AAP) GGCCACGCGTCGACTA GTACGGGIIGGGIIGGGIIG provided with the kit. The amplified fragment was cloned into pCR2.1 TOPO for sequence analysis.

RNA isolation, cDNA probe obtention, and real-time RT-PCR assays. RNA extraction was performed by using an RNeasy kit according to the manufacturer's instructions (Qiagen, Inc., Valencia, CA). Samples were treated with DNase I prior to reverse transcription-PCR (RT-PCR) using the protocol for preparation of DNA-free RNA (Fermentas). cDNA was synthesized from purified total RNA by RT using random primers and reverse transcriptase from the RevertAid H Minus First Strand cDNA synthesis kit (Fermentas). For real-time RT-PCR, TaqMan Universal PCR Mastermix, primer mixes containing a FAM reporter probe, and the gene-specific TaqMan MGB probe (6-FAM dye-labeled) (TaqMan gene expression assay) were obtained from Applied Biosystems. RT-PCR mixtures (25 μl) contained template cDNA, 2× TaqMan Universal PCR Mastermix buffer (12.5 μl), and forward and reverse primers. The optimal primer and probe concentrations and amplification conditions were determined. The forward and reverse *argC* primers and TaqMan probe for each species were added at concentrations of 5 and 2.5 pmol/μl, respectively.

The *S. meliloti rpoA* gene encodes the α subunit of RNA polymerase (RNAP) and is stably transcribed throughout different growth stages. Expression of *rpoA* was used as an endogenous control (normalizer) at concentrations of 1 and 2 pmol/μl. The forward and reverse *gus* primers and TaqMan *gus* probe were

added at concentrations of 5 pmol/μl each. Reactions were analyzed by using an ABI Prism 7300 sequence detector (7300 System SDS, v1.3.0 software; Applied Biosystems). The reaction conditions were as follows: 2 min at 50°C, 10 min of polymerase activation at 95°C, and then 40 cycles of 95°C for 15 s and 55°C for 60 s. Each assay included (in triplicate) a standard curve of six serial dilutions of cDNA. The baseline was corrected by using the default adaptive baseline algorithm, and the threshold was manually adjusted by visual analysis of log-scale amplification plots.

Linear regression analysis was used to calculate the standard curve, estimate the r^2 and slope, and calculate the PCR efficiency (%). After correcting the cycle threshold values (C_T) for amplification efficiency, the expression levels were normalized to the endogenous control, and relative quantification of gene expression was obtained by the comparative C_T method ($2^{-\Delta\Delta CT}$) (47).

Measurement of β-glucuronidase activity. *S. meliloti* cultures were grown to mid-exponential phase in PY medium. Cells were collected by centrifugation at 6,000 × *g* in a Sorvall SS34 rotor, washed with sterile MM, and then concentrated 100-fold. Portions (50 ml) of MM containing 10 mM succinate and 10 mM ammonium chloride as carbon and nitrogen sources, respectively, were inoculated with the cell suspension at an initial OD_{540} of 0.05. Cultures were grown with shaking (200 rpm) for 8 h at 30°C. Quantitative β-glucuronidase activity was measured in a 1.0-ml culture sample using 4-2-nitrophenyl β-D-glucuronide (pNPG) as a substrate (28). The data were normalized to total cell protein concentration obtained by the Lowry method. The specific activities are expressed as nanomoles of *p*-nitrophenol (pNP) per minute per milligram of protein (nmol/min/mg of protein).

Determination of *N*-acetyl-γ-glutamyl phosphate reductase (ArgC) activity. Bacteria were grown in MM. Cell cultures in logarithmic growth phase (8 h for MM with succinate-ammonium or 24 h for MM with mannose-nitrate) were collected by centrifugation and then washed. The cell pellets were resuspended in 5 mM Tris-HCl buffer (pH 7.5), and then the cells were disrupted by sonic oscillation. The supernatant was treated with ammonium sulfate, and the precipitate was discarded. Material that was precipitated by the addition of more ammonium sulfate was collected and dissolved in 5 mM Tris-HCl buffer (pH 7.4), containing 0.6 mM 2-mercaptoethanol. The protein solution was loaded on a Microcon YM-30 column, and the soluble cell extract was collected and used for the measurement of ArgC. The enzymatic activity was measured spectrophotometrically by the disappearance of NADPH in the presence of *N*-acetyl glutamate and ATP. The assay was initiated by adding ArgB (*N*-acetyl glutamate kinase, purified in our laboratory) to the reaction mix since *N*-acetyl glutamyl phosphate, the product of ArgB and substrate of ArgC, is highly unstable and not commercially available. Reaction rates were corrected for NADPH consumption, measured in the absence of added *N*-acetyl glutamate. The specific activity was expressed as nanomoles of NADP produced per minute per milligram of protein. The protein concentration was determined by the Lowry method.

Determination of SpeB activity. For the measurement of agmatine ureohydrolase (SpeB) activity, 150-ml cultures were grown (either for 8 h in MM supplemented with succinate-ammonium or for 24 h in MM supplemented with mannose-nitrate), and the cells were collected by centrifugation. The pellets were washed and then resuspended in 1.0 ml of ice-cold SpeB reaction buffer. The cells were disrupted, and then the cell debris was removed by centrifugation. The supernatant was collected and used to assay SpeB activity. The reaction was stopped by the addition of a perchloric acid solution. The ammonia content in the sample was measured by using a diagnostic urea/ammonia determination procedure (Boehringer Mannheim). The specific activity was expressed as micrograms of ammonia produced per milligram of protein. The protein concentration was determined by the Lowry method.

ArgC proteomic identification and quantification. Bacterial proteins were obtained by sonicating cell cultures (grown 8 h in MM supplemented with succinate-ammonium) for 5 cycles of 1 min each at 4°C in a Vibra Cell (Soniprep150, MSE Sanyo) in the presence of a protease inhibitor (Complete tablets; Roche Diagnostics GmbH, Mannheim, Germany). To further limit proteolysis, protein isolation was performed by using phenol extraction (35). To solubilize and obtain completely denatured and reduced proteins, pellets were dried and resuspended as previously described (21). Prior to electrophoresis, the samples were mixed with 7 M urea, 2 M thiourea, 4% CHAPS {3-[(3-cholamidopropyl)-dimethylammonio]-1-propanesulfonate}, 2 mM tributhyl phosphine (TBP), 2% ampholytes, and 60 mM dithiothreitol. Sample preparation, analytical and preparative two-dimensional polyacrylamide gel electrophoresis (2D-PAGE), and image analysis were performed as previously described (20). pH gradients were obtained using a 2D-PAGE standard (Sigma). For separation in the first dimension, ~500 mg of total protein was loaded. The gels were stained with Coomassie Blue R-250, and protein spots were detected at a 127-by-127-mm resolution using a PDI Image Analysis System and PD-Quest software (Protein Databases, Inc., Huntington Station, NY). Selected spots were excised manually and prepared for mass spectroscopy (MS), as previously described (21). Purified ArgC protein was subjected to enzymatic digestion, and then the resulting peptide fragments were analyzed by complementary MS methods (matrix-assisted laser desorption ionization–time of flight–MS and liquid chromatography-electrospray ionization-tandem MS). ArgC quantification was performed by dot pixel evaluation with PD-Quest software and extrapolated to the total gel load. All experiments were performed three times. Mass spectra were obtained using a Bruker Daltonics Autoflex (Bruker Daltonics, Bellerica, MA) operated in the delayed extraction and reflectron mode. Spectra were externally calibrated using a peptide calibration standard (Bruker Daltonics standard 206095). Peak lists of the tryptic peptide masses were generated and searched against the NCBI nr databases or the Rhizobase (http://bacteria.kazusa.or.jp/rhizo/) using the Mascot search program (Matrix Science, Ltd., London United Kingdom).

Determination of excreted organic acids and amino acids. For extracellular organic acids and amino acids determination, cells were grown for 8 h in MM with succinate-ammonium or 24 h for MM with mannose-nitrate, and 25-ml cultures were subjected to centrifugation, and then the supernatant, free of bacteria, was lyophilized. Amino acids and organic acids were separated and quantified by using reversed-phase high-performance liquid chromatography with a Symmetry C18 column (5 μm, 3.9 by 150 mm; Waters). The data are expressed as nmol/mg of protein and μmol/mg of protein, respectively.

Bioinformatics methods. Codon adaptation index (CAI) calculations were performed with the CAI program in the EMBOSS (European Molecular Biology Open Software Suite) package available at www.emboss.org. The species signature was calculated as the number of specific amino acid residues in the encoded protein that were unique or least abundant at each position based on multiple alignments, and was expressed as a percentage of protein length. Species signatures were calculated with a perl custom program (available on request) based on multiple alignments performed with CLUSTAL W (70). For phylogeny, multiple alignment of translated amino acid sequences was carried out by using MUSCLE v3.7 (17) and the approximate-likelihood rate method with PhyML v3.0 (1, 33) on the Phylogeny.fr server (15). A bootstrap was applied with 100 replicates, and a WAG model for amino acid substitution was used. The tree was drawn with TreeView1.6.6 (Roderic Page). ArgC sequences for species signature evaluation and phylogenetic analysis were obtained from GenBank using the following access numbers: *A. tumefaciens* C58 (NP_354256), *A. vitis* S4 (YP_002549205), *Bradyrhizobium* ORS278 (YP_001205564), *B. melitensis* 16 M (NP_540088), *E. coli* K-12 W3110 (AP_003852), *M. loti* MAFF303099 (Q982X3), *R. etli* CFN42 (ABC90369), and *S. meliloti* 1021 (NP_385346). Obtained *argC* sequences were registered in the GenBank and assigned the following provisional access numbers: *M. loti* strains R88B (HM753558), N86A99 (HM753564), VTI (HM753565), CJ4 (HM753561), CJ2 (HM753562), R12C (HM753559), R7A (HM753560), and CJ6 (HM753563). *S. meliloti* strains Ts48 (HM753568), Cx2 (HM753573), Ter3 1 (HM753570), Mac3 5 (HM753572), REF21 (HM753574), Cx48 (HM753571), SauI 5 (HM753569), Cx26 (HM753575), Tx 30 (HM753567), and ES2 (HM753566). *A. tumefaciens* strains IAM12048 (HM753578), IAM13129 (HM753576), IAM13549 (HM753577), and IAM14040 (HM753579). *R. etli* strains Kim5 (HM753582), CIAT652 (HM753583), GR56 (HM753580), CIAT151 (HM753584), and Brasil5 (HM753581).

RESULTS

Structural analysis of *argC* genes and their protein sequences. (i) Species signatures and phylogenetic relationships of *argC* from *Rhizobiales*. Sequence differences among orthologs could be the result of evolutionary adaptation to a specific cellular environment. The extent of these specific changes has been termed the "species signature" (32). In order to assess the functional importance of species signature in *Rhizobiales*, we focused on a syntenic gene, *argC*, which encodes an *N*-acetyl-γ-glutamyl phosphate reductase that is essential for arginine biosynthesis. Alignment and comparison of the amino acid sequences of ArgC from five species—*R. etli*, *A. tumefaciens*, *S. meliloti*, *B. melitensis*, and *M. loti*—showed that there were 133 positions with identical residues, and 32 (10.3%), 30 (9.6%), 30 (9.6%), and 113 (36.4%) residues, respectively, that were unique and are considered species sig-

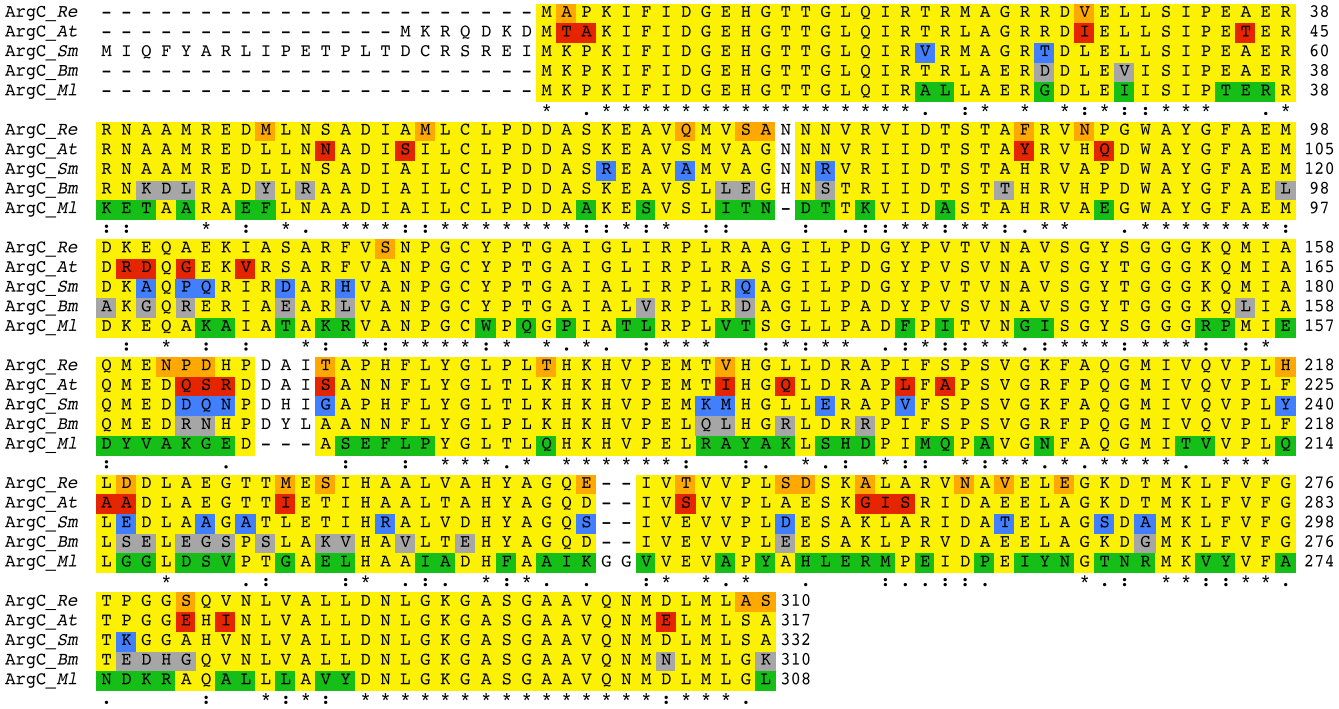

FIG. 1. Species signature of ArgC from *Rhizobiales*. A multiple alignment was carried out using CLUSTAL W. Species signatures were determined with a perl custom script. Yellow blocks indicate identical residues in at least two species. Colored residues for each organism denote species signature as follows: orange, *R. etli*; red, *A. tumefaciens*; blue, *S. meliloti*; gray, *B. melitensis*; and green, *M. loti*. Residues not in blocks are gaps in some organism or nonhomologous sequences.

natures (Fig. 1); the isoelectric points were 5.46, 5.39, 6.0, and 5.4, respectively.

To determine the degree of conservation of the ArgC protein among members of the same species of *Rhizobiales*, the *argC* coding regions of different *Sinorhizobium*, *Rhizobium*, *Agrobacterium*, and *Mesorhizobium* strains were amplified by PCR and then sequenced. The translated sequences showed 98 to 99% similarity among species. A phylogenetic tree was constructed to assess the relationships among *Rhizobiales* species based on the ArgC sequences (Fig. 2). *Rhizobium-Agrobacterium* species exhibited the closest relationships, followed by *Sinorhizobium* strains; *M. loti* sequences were located on a more distant branch. This species relationship was in general concordance with other vertically inherited markers, such as DnaK, GyrB, and AtpD (data not shown).

(ii) Genomic context analysis and identification of the *argC* promoter. The genomic organization of *argC* in *Rhizobiales* was analyzed by using a publicly available annotated database (http://www.ncbi.nlm.nih.gov/genomes/MICROBES). In the circular chromosome in each *Rhizobiales* species analyzed, the *argC* gene are contiguous to upstream *speB* (agmatine ureohydrolase), which participates in the synthesis of putrescine, part of the polyamine synthesis pathway (e.g., spermine and spermidine) involved in several cellular and metabolic functions (37). Previous *in silico* analyses have indicated that *argC* and *speB* are organized in an operon (52, 58).

As an initial approach, the complete putative *speB-argC* operon of each species was cloned and used for complementation analysis of an *S. meliloti argC* mutant (*argC*::ΩSp). The enzymatic activity of ArgC and SpeB expressed from the putative *speB-argC* operons of *S. meliloti*, *A. tumefaciens*, *R. etli*, and *M. loti* was evaluated in the *S. meliloti argC* mutant strain. We found differences in ArgC and SpeB activities (data not shown), which conducted us to consider independent promoters for each gene. To identify the putative *argC* promoter, the *speB-argC* segment-containing plasmids were modified by deletion of 150 bp of *speB* gene using XbaI-KpnI restriction sites (data not shown). Disruption of *speB* did not compromise the ability of the plasmids to complement the mutant phenotype (data not shown).

To verify that there was an independent promoter region for *argC* located within the *speB* coding region, we identified the transcriptional start site of *S. meliloti argC* by 5′RACE using total RNA purified from wild-type strain cells. The *argC* transcriptional start site was located 125 nucleotides upstream of the putative translational start codon, and a putative −10 box characteristic of sigma 70-dependent promoters was identified (see Fig. S1 in the supplemental material).

To determine the transcriptional activity of the putative *argC* promoter of *Rhizobiales*, *argC* promoter-β-glucuronidase (*gus*) gene fusions were constructed, and their activity was evaluated in *S. meliloti* and *M. loti*. As a control, each species-specific promoter-*gus* construct was also evaluated in its native background. As seen in Fig. 3, the activities of the *S. meliloti*, *A. tumefaciens*, and *R. etli argC* promoters were similar in their native backgrounds and in that of *S. meliloti.* Also, the *M. loti argC* promoter had very low activity in the latter background. However, the activities were more induced in the *M. loti* background compared to the *M. loti argC* promoter activity. Thus, the newly identified *argC* promoter was active in all strains, and

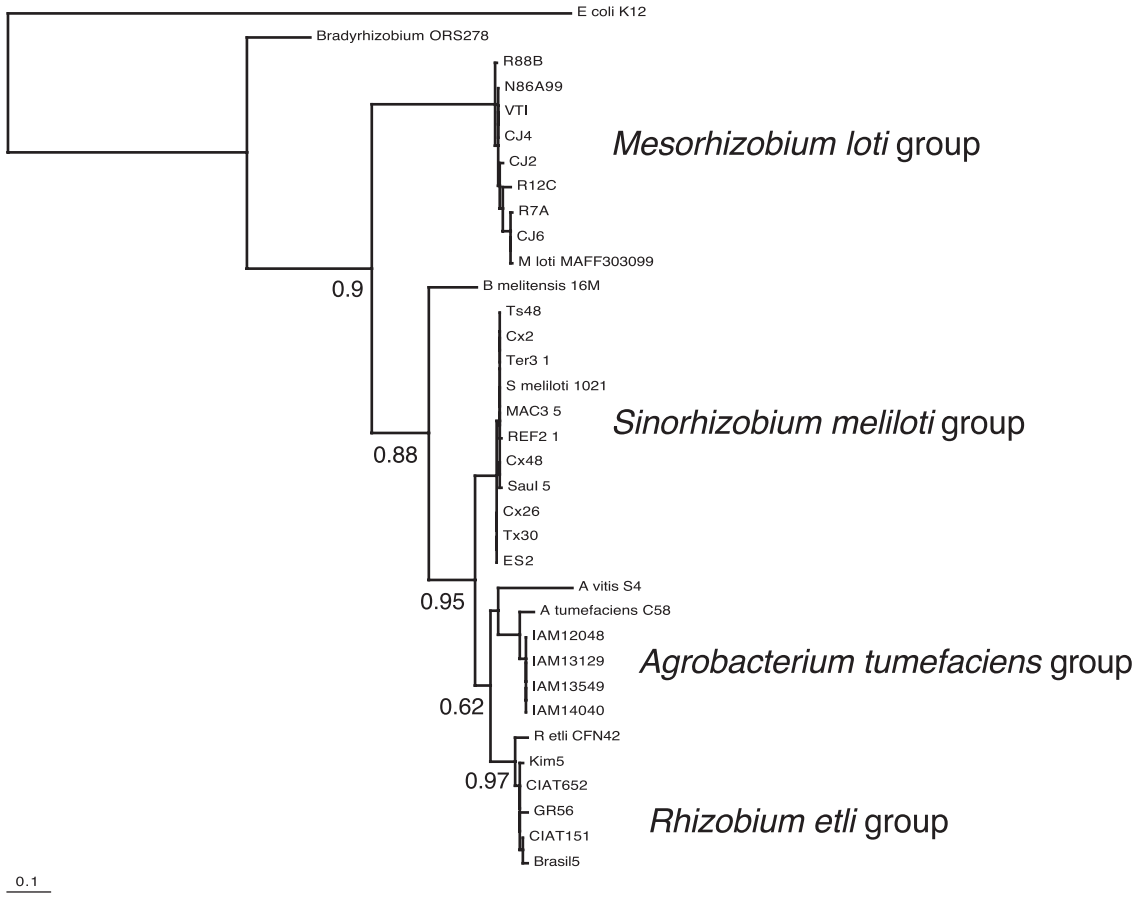

FIG. 2. Phylogenetic analysis of ArgC from *Rhizobiales*. The alignment was done using the MUSCLE program. Phylogeny was generated by the PhyML method. The tree was drawn with TreeView. Bootstrap analysis was performed with 100 replicates. Supporting values are shown in the main branches. The *E. coli* sequence was taken as the outgroup. The bar represents substitutions per residue.

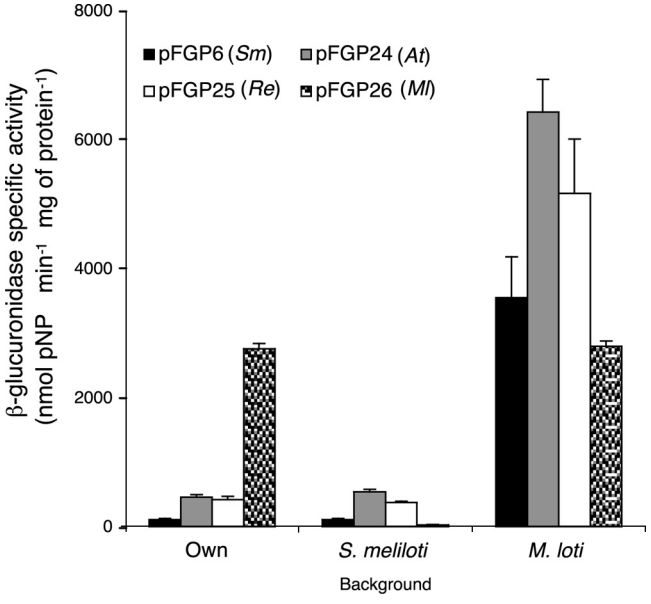

FIG. 3. Transcriptional analysis of *argC* promoter activity. Expression of the indicated *argC* promoter-*gus* (β-glucuronidase) gene fusions is depicted as follows: first group, in the genetic background of the indicated species; second group, in *S. meliloti*; and third group, in *M. loti*. Bars: black, *S. meliloti*; gray, *A. tumefaciens*; empty, *R. etli*; patterned, *M. loti*.

the *M. loti argC* promoter was weakly active in the *S. meliloti* background.

The species signatures of *Rhizobiales* ArgC orthologs ranged from 10 to 36%, and phylogenetic analysis revealed that *R. etli* was closely related to *A. tumefaciens*. Unique to *Rhizobiales*, the *argC* gene is linked to *speB* (involved in putrescine synthesis), and in the case of *S. meliloti* it was demonstrated that *argC* has its own active promoter inside the coding sequence of *speB*. *M. loti argC* promoter activity was very low in the *S. meliloti* background compared to its native background.

Expression analysis of *argC* regulated by different promoters. The aim of the present study was to determine the complementation efficiency of *argC* orthologs from related species in an *S. meliloti argC* mutant. The level of mRNA synthesis is dependent on promoter activity; thus, we were interested in the expression patterns of the Rhizobiales *argC* genes under the control of the same promoter, either the *S. meliloti speB* (p*speB*) promoter, the *S. meliloti argC* (p*argC*) promoter, or the *E. coli lac* (p*lac*) promoter.

The level of expression of β-glucuronidase under the control of the *lac* promoter was three times higher than the *S. meliloti argC* promoter (compare the first and second lines in Table S2 in the supplemental material). In contrast, the *S. meliloti speB* promoter exhibited very low activity under the same conditions

TABLE 2. Effect of *argC* gene sequences on transcriptional expression

Sequence in fusion	Mean β-glucuronidase sp act ± SD[a]			
	S. meliloti	*A. tumefaciens*	*R. etli*	*M. loti*
ATG	233 ± 15	210 ± 28	230 ± 39	249 ± 17
Partial CDS (100 bp)	366 ± 23	284 ± 30	206 ± 25	637 ± 131
Partial CDS (880 bp)	439 ± 51	319 ± 48	270 ± 48	591 ± 103
Complete CDS	145 ± 6	280 ± 30	30 ± 3	153 ± 7

[a] Values are expressed as nmol of *p*-nitrophenol min^{-1} mg of $protein^{-1}$. Data represent the means of two replicates from three independent experiments. The expression under p*argC*$_{Sm}$ was determined.

(26- and 8-fold less than p*lac* or p*argC*, respectively) (third line in Table S2 in the supplemental material). These results indicated that in *S. meliloti*, p*lac* is a strong promoter, whereas p*argC* and p*speB* are moderate and weak promoters, respectively. For a comparative analysis, we used these promoters to drive the expression of *argC* from *A. tumefaciens*, *S. meliloti*, *R. etli*, and *M. loti*. The levels of transcriptional activity from the different promoters were similar to those obtained above (data not shown).

To determine the transcriptional activity through the *argC* sequences, we analyzed the expression of transcriptional fusions either containing the complete *argC* sequence, containing a partial *argC* sequence (either with 880 or 100 bp), or lacking the coding region completely (containing only the ATG codon) under the control of the *S. meliloti argC* promoter. Constructs were analyzed in an *S. meliloti* wild-type strain background. Deletion of *argC* gene portions had variable effects on transcription rates, resulting in increased reporter gene expression in the first 100 to 880 bp of the gene (Table 2). The effect was more drastic with *M. loti argC* (an ~2.5-fold increase compared to the start codon alone), followed by *S. meliloti* (2-fold increase) and *A. tumefaciens* (50% increase). The exception was the *R. etli argC*, whose activity was similar for the truncated sequences and the start codon alone. Interestingly, expression was drastically reduced when the complete *argC* gene sequence was evaluated, indicating sequences with a stalling effect on transcription. The expression of *R. etli argC* was nearly constant with shorter versions, but with the complete gene sequence the effect was very strong. These results suggested that, at least in plasmid, the *argC* coding region itself can influence gene expression, in agreement with other recent results about gene sequences modulating their transcription-translation rates (27, 43). Codon adaptation index (CAI) values were calculated for each *argC* gene in the *S. meliloti* background and yielded values ranging from 0.76 to 0.8.

Plasmid copy number also can play an effect in expression of genes; therefore, we assessed *argC* gene copy using plasmid with p*speB* promoter and chromosomal *rpoA* as a control. The control plasmid (vector alone) was present in cells at approximately two plasmid copies per chromosome (1.8 ± 0.17), as were the *R. etli* (2.1 ± 0.18), *A. tumefaciens* (2.3 ± 0.1), and *S. meliloti* (2.9 ± 0.11) gene-containing plasmids. In contrast, the *M. loti* gene-containing plasmid was present at 9.2 ± 0.23 plasmid copies per chromosome.

Based on *gus* reporter gene expression analysis, we were able to characterize three promoters of various strengths: weak (*S. meliloti* p*speB*), intermediate (*S. meliloti* p*argC*), and strong (*E. coli* p*lac*). Differential transcriptional regulation of complete and partial gene sequences suggested that *argC* coding sequences may modulate their transcriptional rates. An additional mechanism exists that modulated the plasmid copy number in the case of *M. loti argC* ortholog complementation.

Complementation analysis of *argC* from *Rhizobiales* under different promoters. (i) Physiological analysis: growth, duplication times, and excretion of metabolites. The optimal growth conditions for *S. meliloti* wild-type strain was MM containing succinate-ammonium, and typical doubling times were 3 h (Fig. 4). We also investigated suboptimal growth conditions in order to differentiate complemented strains. In MM containing mannose-nitrate, the wild-type strain exhibited delayed growth, with a doubling time of 6 h. Under either set of conditions, the *argC* mutant strain failed to grow. The best complementation was achieved with *argC* under the control of p*argC* (Fig. 4A and B). Under that promoter in both MM growth conditions, all complemented strains grew at similar rates and to levels similar to that of the wild-type strain, and similar duplication times were obtained. Under the control of p*lac*, under both sets of conditions, the growth of all complemented strains was similar to that of the *S. meliloti* wild-type strain (Fig. 4C and D). The *A. tumefaciens*-complemented strain exhibited delayed growth, with increased duplication times of 4 and 8 h in succinate-ammonium and mannose-nitrate, respectively. Under the control of p*speB* (from *S. meliloti*), the complemented strains exhibited reduced growth under both sets of conditions. The *R. etli*- and *A. tumefaciens*-complemented strains exhibited reduced growth, increased duplication times (8 h), and long lag phases (Fig. 4E and F); the *M. loti*-complemented strain failed to grow. Only *S. meliloti*-complemented strain growth was similar to that of the wild type.

Given the limited growth of the complemented strains when *argC* was placed under the control of p*speB* (Fig. 4E and F), we investigated the concentration of metabolites excreted into the culture medium, possibly as a response to a faulty metabolism. In MM containing succinate-ammonium, the *argC* mutant strain excreted 6 to 15 times more glutamate and glycine compared to the wild-type strain, 15 times more α-ketoglutarate, and consumed only a fraction of the succinate consumed by the wild-type strain (Table 3). These levels were restored to wild-type levels when the mutant strain was grown in MM supplemented with arginine. The *S. meliloti*-complemented strain exhibited the most wild-type-like metabolic profile, while the *R. etli*- and *A. tumefaciens*-complemented strains excreted slightly more α-ketoglutarate and consumed a little less succinate, than the rest of complemented strains (Table 3). The *M. loti*-complemented strain showed the highest levels of excreted metabolites, even compared to the *argC* mutant strain (twice the level of glutamate and more than 50% more α-ketoglutarate compared to the *argC* mutant). In MM containing mannose-nitrate, higher glutamate and glycine levels were observed for the mutant strain, compared to MM containing succinate-ammonium, as well as a reduction in the excreted levels with the addition of arginine. The complemented strains showed differential behavior compared to MM with succinate-ammonium. The *S. meliloti*- and *R. etli*-complemented strains showed 10-fold reduction of glutamate excretion, while the *A. tumefaciens*- and *M. loti*-complemented strains showed a slight increase. For glycine excretion, a severalfold increase was

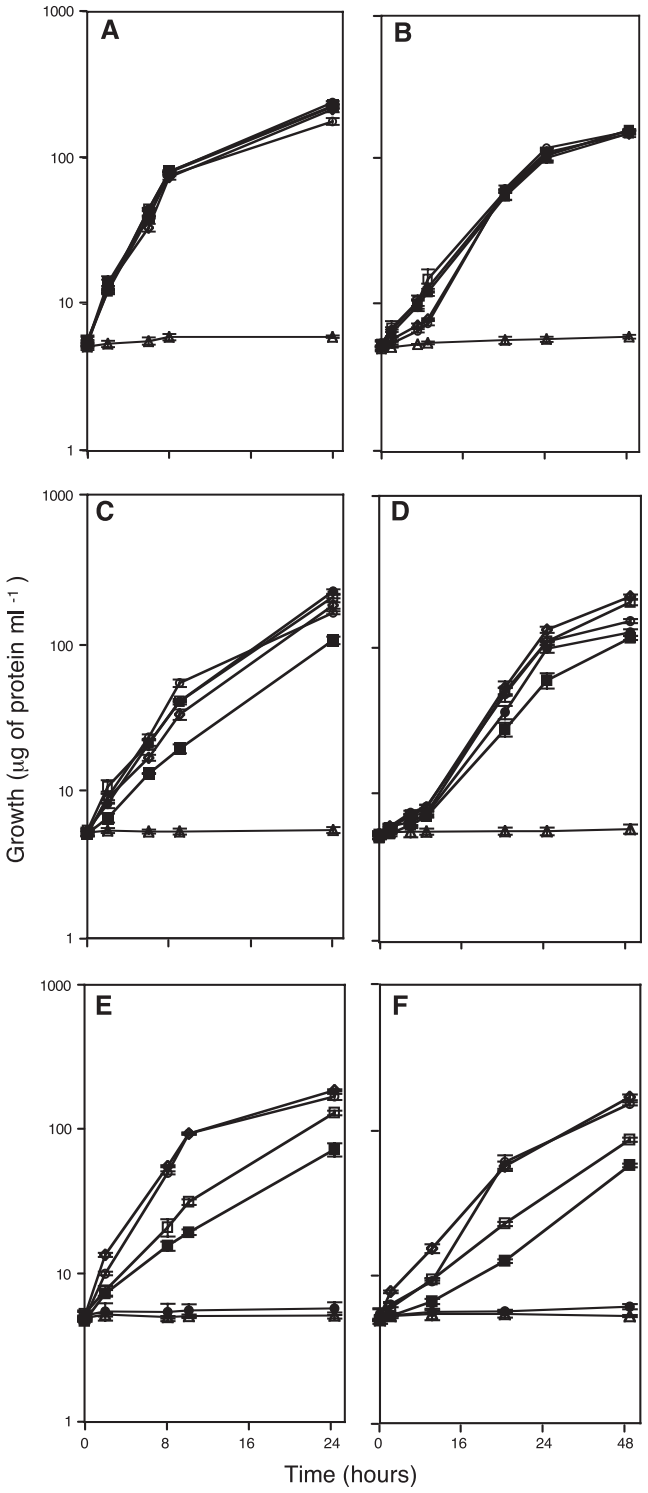

FIG. 4. Growth curves of *S. meliloti argC*-complemented strains. The left panels depict growth in MM supplemented with 10 mM succinic acid and 10 mM ammonium chloride. The right panels depict growth in MM supplemented with 10 mM mannose, 10 mM potassium nitrate. (A and B) *argC* under the control of the *S. meliloti argC* promoter; (C and D) *argC* under the control of the *E. coli lac* promoter; (E and F) *argC* under the control of the *S. meliloti speB* promoter. Each panel represents the *argC* mutant strain complemented with *argC* gene from *S. meliloti* (◆), *A. tumefaciens* (■), *R. etli* (□), and *M. loti* (●); the *S. meliloti* wild-type strain (○); and the *argC* mutant strain (▲).

observed for all of the complemented strains and was drastic with the *M. loti* gene. In the case of α-ketoglutarate, there was a slight reduction for the *S. meliloti* gene and the reduction was approximately 50% in the rest of complemented strains.

These results clearly demonstrated that the *argC* promoters and gene sequences were important determinants of growth capacity in the complemented strains. The newly identified *argC* promoter was optimum for all strains, followed by the strong, constitutive *lac* promoter. There were clear differences among the phenotypes of strains complemented with *A. tumefaciens*, *R. etli*, and *M. loti argC* under the control of p*speB*, none of which fully complemented the *argC* mutant phenotype.

(ii) Biochemical characterization of complemented strains: ArgC and SpeB enzymatic activity. We evaluated the *N*-acetyl-γ-glutamyl phosphate reductase (ArgC) of strains containing plasmids with promoter-*argC* constructions and compared the results to the growth phenotype. The wild-type strain showed reduced activity and, compared to the *S. meliloti*-complemented strain, the multicopy effect was apparent again, in diverse proportions, with the exception of construct under p*speB* promoter (Table 4). Complemented strains grown in MM supplemented with mannose-nitrate showed a reduction in ArgC activity in almost all cases, except for *S. meliloti* under p*lac* and *A. tumefaciens* in the *speB-argC* construct. The tendency toward reduced activity was possibly because these compounds are poor carbon and nitrogen sources for *S. meliloti*.

Under the control of p*argC*, in MM containing succinate-ammonium, the *S. meliloti*-complemented strain had the highest enzymatic activity, and the *M. loti*-complemented strain had the lowest. In MM containing mannose-nitrate, similar proportions among the strains were observed (Table 4). These activity levels were sufficient for all of the strains to achieve optimal growth (see Fig. 4A and B).

Under both growth conditions, p*lac* conferred high activity levels, most notably in the *S. meliloti*-complemented strain (Table 4). In this case, the growth delay of the *A. tumefaciens*-complemented strain did not correlate with diminished activity. Under the control of p*speB*, there was reduced ArgC activity in all strains (Table 4). In the *M. loti*-complemented strain, this level of activity was insufficient to support growth (see Fig. 4E and F). In addition, although both *R. etli*- and *A. tumefaciens*-complemented strains exhibited similar activity levels in terms of complementation of the *argC* mutant phenotype in MM containing succinate-ammonium compared to the *S. meliloti*-complemented strain, they did not grow well and had long lag phases in MM containing mannose-nitrate.

Strains containing the construct *speB-argC* (with each gene expressed from its own promoter) showed similar growth compared to wild-type (not shown) and intermediate ArgC activity levels (Table 4)—with the exception of the *M. loti*-complemented strain, which did not grow in both MM conditions and showed very reduced ArgC activity (Table 4). The activity of SpeB was also evaluated for strains with the *speB-argC* construct, and similar levels of activity were found among the complemented strains in both growth conditions (Table 4).

Plasmids with *S. meliloti* and *M. loti argC* genes also were introduced into the *S. meliloti* wild-type strain, and no differences in ArgC activity were observed in MM supplemented with succinate-ammonium, with the exception of *M. loti*-complemented strain under p*speB*, that presented one-third reduc-

TABLE 3. Metabolite excretion of *S. meliloti argC* complemented strains under the *S. meliloti* p*speB* promoter

Strain	Metabolite excretion (mean ± SD)[a]						
	MM succinate-ammonium (8 h)				MM mannose-nitrate (24 h)		
	Glu*	Gly*	α-Kg†	Succ†	Glu*	Gly*	α-Kg†
S. meliloti							
1021 wild type	1.6 ± 0.7	0.1 ± 0.1	13.6 ± 1.0	226.6 ± 25.2	0.1 ± 0.2	12.6 ± 2.0	10.4 ± 0.8
argC mutant	7.1 ± 3.3	1.5 ± 0.1	228.6 ± 74.0	3356.6 ± 1201.2	24.6 ± 0.5	396.4 ± 78.2	129.2 ± 36.3
argC mutant (+1 mM Arg)	0.2 ± 0.1	0.4 ± 0.2	11.7 ± 0.7	176.8 ± 1.2	0.4 ± 0.3	3.6 ± 0.8	9.2 ± 4.8
argC mutant complemented strains							
pFGP16 (*S. meliloti*)	1.0 ± 0.2	0.8 ± 0.1	13.3 ± 0.9	235.6 ± 23.0	0.1 ± 0.5	54.4 ± 13.0	11.3 ± 1.2
pFGP17 (*A. tumefaciens*)	6.5 ± 0.3	0.6 ± 0.1	68.5 ± 3.9	1246.0 ± 93.9	11.4 ± 2.4	183.4 ± 74.9	40.6 ± 4.6
pFGP18 (*R. etli*)	1.1 ± 0.3	0.5 ± 0.1	53.7 ± 3.8	854.8 ± 38.7	0.1 ± 0.2	168.2 ± 17.9	19.7 ± 2.7
pFGP19 (*M. loti*)	15.9 ± 2.4	1.6 ± 0.4	328.4 ± 11.6	5217.9 ± 1841.0	18.4 ± 0.3	898.0 ± 10.6	151.6 ± 8.4

[a] Glu, glutamate; Gly, glycine; α-Kg, α-ketoglutarate; Succ, succinate. *, Expressed as nmol mg of protein^{-1}; †, expressed as μmol mg of protein^{-1}.

tion in the activity (not shown). This was possibly due to the formation of slightly inefficient ArgC hybrid multimers that reduced native activity.

With the exception of strains carrying the p*speB* promoter in MM containing succinate-ammonium, there was a good agreement between growth curves and ArgC activity. Optimal growth and high ArgC activity were obtained with p*argC* and p*lac*. In the case of p*speB*, the *M. loti*-complemented strain showed the lowest complementation efficiency and a no-growth phenotype. *R. etli*- and *A. tumefaciens*-complemented strains under the p*speB* promoter exhibited similar enzymatic activities compared to the *S. meliloti*-complemented strain; however, they showed severe growth delay.

(iii) Molecular analysis: *argC* transcript levels, direct ArgC quantification, and translational index. Given the results of the analysis of ArgC activity and growth phenotype, we next investigated important factors influencing the ability of orthologous *argC* genes to complement the *S. meliloti argC* mutant phenotype, such as mRNA production and translational efficiency in strains containing the pBBMCS53 vector, carrying the *argC* and *gus* genes, which permitted the complementation and monitoring of transcription simultaneously (see Materials and Methods). The mRNA level in the wild-type strain was used as the reference and given a value of 1.0. The ArgC protein was quantified directly by two-dimensional gel electrophoresis and mass spectrometry. The mRNA levels and the amount of protein detected by proteomic identification were used to calculate a translational efficiency index (proteomic protein/mRNA).

The wild-type strain exhibited nearly constant values for mRNA, proteomic protein, and translational index in each set of assays (Table 5). In general, the *S. meliloti*-complemented

TABLE 4. ArgC and SpeB specific activities of *S. meliloti argC* complemented strains under the control of different promoters

Protein and conditions	Mean ArgC and SpeB sp act ± SD[a] of *argC* mutant complemented strains[a]				
	WT	*S. meliloti*	*A. tumefaciens*	*R. etli*	*M. loti*
ArgC					
p*argC* (pFGP12 to pFGP15)					
Succinate-ammonium	16.6 ± 0.4	134.0 ± 2.6	80.1 ± 2.3	83.1 ± 1.4	13.3 ± 0.8
Mannose-nitrate	16.3 ± 0.4	68.8 ± 0.9	28.7 ± 1.4	32.3 ± 1.9	7.1 ± 0.3
p*lac* (pFGP8 to pFGP11)					
Succinate-ammonium	16.7 ± 0.3	405.4 ± 3.4	49.0 ± 1.5	59.5 ± 0.9	60.6 ± 0.7
Mannose-nitrate	16.4 ± 0.1	432.4 ± 20.7	81.7 ± 2.8	32.1 ± 3.1	81.9 ± 8.7
p*speB* (pFGP16 to pFGP19)					
Succinate-ammonium	16.7 ± 0.3	20.8 ± 0.4	19.3 ± 0.5	18.9 ± 1.3	0.8 ± 0.2
Mannose-nitrate	16.1 ± 0.3	25.0 ± 0.1	16.6 ± 0.1	17.7 ± 0.1	0.9 ± 0.1
speB-argC (pFGP1 to pFGP4)[b]					
Succinate-ammonium	14.5 ± 0.3	102.6 ± 7.4	107.5 ± 3.9	38.0 ± 6.6	0.8 ± 0.2
Mannose-nitrate	16.2 ± 0.1	57.3 ± 10.3	115.4 ± 1.7	35.2 ± 0.8	1.0 ± 0.1
SpeB[c]					
speB-argC (pFGP1 to pFGP4)					
Succinate-ammonium	6.5 ± 0.1	39.9 ± 6.1	53.2 ± 2.3	55.1 ± 1.9	62.2 ± 1.2
Mannose-nitrate	9.2 ± 0.1	46.6 ± 3.4	43.7 ± 3.4	38.9 ± 1.6	21.5 ± 6.6

[a] Expressed as nmol of NADP min^{-1} mg of protein^{-1}, except as noted (see footnote *c*). WT, *S. meliloti* 1021 wild-type strain.
[b] That is, constructs containing *speB* and *argC* under their own promoters.
[c] Expressed as μg of ammonia mg of protein^{-1}.

TABLE 5. mRNA, protein quantification, and translational efficiency index for *S. meliloti argC* mutant complemented strains

Promoter and parameter[a]	*argC* mutant complemented strains[b]				
	WT	*S. meliloti*	*A. tumefaciens*	*R. etli*	*M. loti*
p*argC* (pFGP12 to pFGP15)					
mRNA	1	9.4 ± 0.5	51.1 ± 4.8	127.6 ± 22.4	19.9 ± 0.4
Proteomic protein	9.8 ± 0.5	771.2 ± 91.1	442.7 ± 20.8	331.6 ± 29.9	273.6 ± 58.8
TEI	9.8	82.0	8.7	2.6	13.8
p*lac* (pFGP8 to pFGP11)					
mRNA	1	121.4 ± 11.8	1,759.2 ± 68.2	1,596.7 ± 69.7	1,598.7 ± 42.9
Proteomic protein	9.5 ± 0.1	1,834.2 ± 100.3	1,399.5 ± 213.2	91.7 ± 26.9	1,696.1 ± 303.1
TEI	9.5	15.1	0.8	0.1	1.1
p*speB* (pFGP16 to pFGP19)					
mRNA	1	4.9 ± 0.6	53.1 ± 2.9	35.0 ± 1.1	162.9 ± 9.5
Proteomic protein	9.5 ± 0.1	25.1 ± 0.1	65.5 ± 2.8	72.9 ± 7.9	67.4 ± 5.2
TEI	9.5	5.1	1.2	2.1	0.4

[a] mRNA values were normalized relative to the abundance of mRNA in the wild-type strain. Proteomic protein was quantified by using spectrometry and dot pixels. TEI, translational efficiency index (proteomic protein/mRNA).
[b] WT, *S. meliloti* 1021 wild-type strain. Cells were grown for 8 h in MM supplemented with 10 mM succinic acid and 10 mM ammonium chloride.

strain obtained the best translational efficiency index values in each condition compared to the rest of the strains. Also, despite the fact that *argC* orthologs were controlled by the same promoter in each set, different amounts of mRNA and protein were produced, confirming the findings regarding the transcriptional effect of *argC* coding sequences detected with *gus* fusions (see Table 2).

In the case of expression driven by p*argC* promoter, the *S. meliloti*-complemented strain had 10 and 78 times more mRNA and ArgC protein production, respectively, than the wild-type strain, and an 8-fold increase in translational index (Table 5). The levels of mRNA in the other complemented strains were in the range of 20- to 140-fold higher than in the wild type, and yet the translational index in these strains was lower, with the *R. etli*-complemented strain having the lowest translational index. Despite these variations, all strains exhibited similar growth efficiency.

When strains were controlled by p*lac* promoter they exhibited highly elevated levels of mRNA. In the *S. meliloti*-complemented strain, there was an almost 110-fold increase in mRNA compared to the wild-type strain; mRNA levels in the other complemented strains increased more than 1,500-fold (Table 5). A similar trend in high protein levels was observed, with the exception of the *R. etli*-complemented strain, which also had the lowest translational index in this set. The *S. meliloti*-complemented strain demonstrated the highest protein level, but because its mRNA was so much lower, it had the highest translational index.

In the last set, strains with *argC* expression under the p*speB* promoter exhibited the lowest values of mRNA and proteomic protein production. The complemented strains showed mRNA increases of 5-fold (*S. meliloti*), 7-fold (*R. etli*), 11-fold (*A. tumefaciens*), and 30-fold (*M. loti*) compared to the wild-type strain. However, the last three strains showed similar levels in proteomic protein (a 7-fold increase compared to the wild type) and very low translational index values.

Another complete set of constructs was obtained with pBBR1MCS3 and *argC* alone (without *gus* reporter). Similar values and proportions among the strains were found in comparison to the set of strains described above (data not shown). However, strains with pBBR1MCS3 showed slightly increased duplication times, and some reduced ArgC activity (not shown). It is possible that *gus* fused to *argC* genes produced some type of stabilization.

The described molecular parameters, together with the translation/transcription index, provided relevant information about the functional performance of the complemented strains, which demonstrated that complementation of ArgC with the *S. meliloti argC* gene in its own background showed the highest translational index (Table 5), followed by those with the *R. etli* and *A. tumefaciens* orthologs.

DISCUSSION

The species signature was intended to extract the amount of particular specific amino acid residues in positions of multiple alignments of the orthologous protein sequences (32). In this context, the species signature denotes the change in physicochemical properties of the proteins and displays certain particular characteristics of the orthologous products. It is relevant because the sequence differences of the orthologs are translated into amino acid residues; we wanted to establish whether these differences can be studied by ortholog complementation and functional performance when compared in the same cellular background and related to wild-type complementation and wild-type strain.

We studied the *argC* gene because it forms part of an importantly compromised pathway that is central to amino acid and protein synthesis; also, arginine has the highest nitrogen content among the amino acids, its synthesis demands a huge amount of energy, and it is a precursor for polyamine synthesis (14, 48, 63, 68). The *S. meliloti argC* gene was mutated in the chromosome, and then the complementation was obtained either with its own gene or with the ortholog from closely *Rhizobiales* species; they were cloned on the same vector and expressed under the same promoter to study the ability to recover the arginine prototrophy.

Three promoters were used in order to achieve diverse ex-

pression degrees, and we found strong (p*lac*), medium (p*argC*), and weak (p*speB*) transcriptional levels (see Table S2 in the supplemental material). That from *speB* was used because the gene is upstream to *argC* in *Rhizobiales* and participates in polyamine synthesis (e.g., arginine utilization), which is important in diverse metabolic processes but not so abundant as amino acids (68). With these promoters we searched expression levels similar to those of the wild-type strain. In the case of *argC* complementation under the p*speB* promoter, we obtained the lowest ArgC specific activity and major differences, in regard to the optimal maintenance of cellular growth: the gene sequences from *R. etli* and *A. tumefaciens* showed reduced growth ability and that from *M. loti* showed no growth (Fig. 4E and F).

Interestingly, diverse factors altered the expression of the *argC* orthologous sequences and their complementation ability in several levels. In the first level, there was a differential multicopy effect due to plasmid vectors, because under the *speB* promoter we found two to three plasmid copies with *S. meliloti*, *R. etli*, and *A. tumefaciens* sequences, but nine copies with the *M. loti* gene. The most divergent sequence from *S. meliloti* was precisely that from *M. loti*, and the complemented strain carrying this gene presented marked inability to recover arginine synthesis and restore cell growth (Fig. 4E and F). The increased plasmid copy number was possibly related to a gene dosage compensation to favor abundance of the gene, as observed in other bacteria (67) and eukaryotes (18). Lind et al. (46), in a recent report dealing with orthologous replacement of ribosomal proteins in *Salmonella enterica* serovar Typhimurium, found that gene amplification is a compensatory mechanism to restore fitness decay. In our results, despite increase in gene copy number, growth was not fully recovered. Lind et al. showed that gene amplification is important for horizontally transferred genes and the evolution of new functions from gene duplication.

In the next level—transcription of the orthologous genes—also was affected. Theoretically, different genetic sequences located downstream of the same promoter will have the same level of transcriptional activity. However, the *argC* coding sequence itself appeared to modulate transcription to a certain extent (Tables 2 and 5). This may be due to codon usage (but in this case similar CAI values were obtained, and thus codon usage apparently did not play a role in complementation efficiency), codon distribution (8), interaction of translation factors with RNA polymerase and ribosome (7, 59), and the formation of mRNA secondary structures that can alter the speed of the transcriptional complex. Other authors have made the same observation, at the level of transcription-translation processes (43). In addition, as reported recently, important transcription modulation occurs in the first and last 100 nucleotides of the genes (71). A similar effect was clearly observed in transcriptional fusions with segments of genes (Table 2) and also when expression was directly quantified by RT-PCR (Table 5), because under each of the three promoters different amounts of synthesized mRNA were found for each *argC* gene.

The previously described effects on transcription-translation processes, altogether with coding sequence differences of the orthologs (the species signature), consequently affected enzymatic activity of ArgC (Table 4), having a physiological repercussion on growth rate (Fig. 4) and metabolite excretion to the culture medium (Table 3). The diminished growth rate is related to intermediary metabolites that cannot be completely assimilated and are excreted in huge amounts (19). To perform an in-depth analysis of what was occurring in the complementation assay, we decided to measure molecular parameters such as direct mRNA and protein quantification (Table 5) to obtain a translational efficiency index; these parameters helped to clarify the transcriptional-translational ability of *argC* genes cloned on plasmids.

The *S. meliloti* wild-type strain showed the best translational efficiency, with almost constant values; this reproducibility supported the reliability of our approach (Table 5). In the complementation with the *S. meliloti* gene under the p*speB* promoter, the copy number effect was evident, since a 5-fold increase in the mRNA amount was found, compared to the wild-type strain. However, this value did not correlate directly with the copy number found (i.e., 2.9), so possibly something else influenced the transcription rate, such as the supercoiling state of the replicon (24).

Under the p*lac* promoter, the highest amounts of transcripts were obtained, but not the maximum translational efficiency indexes. It was apparent that there is a translational limit in the cell. In this case, the *R. etli*-complemented strain obtained the lowest index, however, it was sufficient to promote an adequate growth recovery (Fig. 4C and D). Under the p*speB* promoter, despite the fact that the *M. loti*-complemented strain showed more gene copies, that amount was not enough to sustain cell growth, possibly because cells had a low translation efficiency index (Table 5 and Fig. 4E and F). It is important to note the lack of correlation between protein synthesis and enzymatic activity, which was very marked in the case of p*lac* constructs. We believe that there exists a physiological limitation to reaching high levels of enzymatic activity, a limitation that was exerted mainly in the case of *Rhizobiales* complementing sequences (because the *S. meliloti* sequence indeed showed a high level of ArgC activity under p*lac*). Several other enzymatic and physiologic factors may participate and alter the correlation between transcription and translation activity (such as stoichiometry, cofactors, regulators, enzymes of the pathway, energy flux, etc.). Another consideration is that activity was measured *in vitro* and that this does not completely reflect the physiologic alteration of *argC* ortholog expression. We thus consider that cellular growth was a more faithful measure of what occurred with ortholog complementation.

The ArgC proteins from *S. meliloti*, *R. etli*, and *A. tumefaciens* displayed similar amounts of species signature differences (ca. 10%), which was indicative of their phylogenetic proximity. Sequences from *B. melitensis* and *M. loti* were evolutionarily more distant (Fig. 2), and the species signatures were higher (36% for *M. loti*) (Fig. 1). We sequenced the *argC* gene from several strains of each species (with the exception of *Brucella melitensis*), and the phylogenetic relationships between these sequences helped to define clear species clusters (Fig. 2). The genomic organization of *argC* genes in *Rhizobiales* was very unusual, since this gene was closely linked to *speB* (from the polyamine synthesis pathway). Possibly, these genes have independent promoters and mechanisms of transcriptional regulation, with the ability to respond appropriately and effectively to particular regulatory signals.

Transcriptional activation by species-specific *argC* promot-

ers was also characterized in the native background and in *S. meliloti* and *M. loti*. In the native backgrounds, the lowest activity was seen in *S. meliloti*, the highest was seen in *M. loti*, and the other species were intermediate (Fig. 3). Interestingly, the *argC* promoter from *M. loti* was not active in *S. meliloti*; in contrast, the *argC* promoters of all of the strains were highly active in *M. loti* (Fig. 3). A partial growth defect was also apparent in the *A. tumefaciens*- and *R. etli*-complemented strains when the expression of *argC* was driven by the *speB* promoter (Fig. 4E and F). This partially defective growth phenotype correlated with a slight increase of α-ketoglutarate excretion to the culture medium and less utilization of succinate in comparison with the wild-type strain (Table 3). A similar phenotype was observed for a GOGAT mutation in *R. etli* (10).

Orthologous genes encode the same function (although some differences have been described for the HoxA3 ortholog in mice and zebrafish) (11), but they may also contain sequence characteristics that reflect specific adaptations. The specific sequence differences in a gene alter the physicochemical characteristics of the encoded proteins and may affect protein function. Factors such as transcription and translation rates, enzyme kinetics, transcriptional regulation, intracellular environment, availability of substrates, and interacting metabolites, proteins, and ions could also affect performance (30, 39, 55, 72).

Species adaptation is a slow process. Neutral drift (point mutations) and natural selection produce numerous changes in a gradual manner, each change having a small effect on fitness. However, some changes can have vast effects on an organism and tend to outcompete small-effect mutations. It has been generally accepted that any attempt to discern these changes experimentally is futile (12). Despite the fact that "species" differentiation in bacteria is considered imprecise, and its existence is even debatable (26, 44), homologous recombination and point mutations can gradually convert a homogeneous bacterial population into different, nonrecombinable populations. In this way, small (neutral and almost neutral) and large (non-neutral) genetic changes could eventually result in a new species. It remains to be seen whether the elemental mechanisms for adaptation, considered microevolution, can reconstruct the higher processes of macroevolution, including speciation and the emergence of biodiversity (12). The appearance of a new phenotype, such as citrate utilization in the presence of oxygen by an *E. coli* population in Lenski's long-term experiment, is something close to speciation (2, 5). However, even random variation (bet hedging) can enhance long-term fitness by increasing the likelihood of individuals to express an adaptive phenotype (3). There is a general lack of knowledge of how ortholog replacement may affect cell functioning and fitness. In this regard, the present study is a valid approach to sorting out the diverse consequences of expression in one species of orthologous sequences from other related species, in which specific amino acid changes may have been derived through adaptation.

In the present study we have demonstrated that an in-deep complementation analysis can uncover unusual complexity. We evaluated the ability of ArgC orthologs from closely related Rhizobiales species containing specific sequence differences to physiologically complement the *S. meliloti argC* mutant phenotype. We observed many factors participating in the complementation efficiency of each ortholog. In addition, we identified a novel promoter for *argC* in Rhizobiales, the presence of which was not predicted by existing genomic information. In agreement with recent reports (27, 43), we demonstrated that coding sequences participate in the regulation of transcription and translational efficiency, perhaps modulating mRNA stability through the formation of secondary structures. Altogether, these are important findings that open new research perspectives.

ACKNOWLEDGMENTS

This study was partially supported by the Dirección General de Asuntos del Personal Académico (DGAPA-Universidad Nacional Autónoma de México), grants IN215307 and IN212710, and by the Ph.D. Program in Biomedical Sciences-UNAM.

We thank Mario Alberto Flores for help in the construction of the *S. meliloti argC* mutant; Michael Dunn for ArgB purification; Sandra Contreras, Miguel Elizalde, Magdalena Hernández, and Gabriel Martínez-Batallar for metabolite and proteome determinations; Gabriela Guerrero and Alejandro Aguilar for preparation of graphs; Ricarda Rivero, Yunuen Acevedo, and Alma Reyes (CCG-UNAM) for technical assistance; and Claudia Silva (IBt-UNAM) and Clive Ronson (Otago University, Otago, New Zealand) for the donation of strains.

REFERENCES

1. **Anisimova, M., and O. A. Gascuel.** 2006. Approximate likelihood ratio test for branches: a fast, accurate and powerful alternative. Syst. Biol. **55:**539–552.
2. **Barrick, J. E., S. Y. Yu, S. H. Yoon, H. Jeong, T. K. Oh, D. Schneider, R. E. Lenski, and J. F. Kim.** 2009. Genome evolution and adaptation in a long-term experiment with *Escherichia coli*. Nature **461:**1243–1247.
3. **Beaumont, H. J. E., J. Gallie, C. Kost, G. C. Ferguson, and P. B. Rainey.** 2010. Experimental evolution of bet hedging. Nature **462:**90–93.
4. **Better, M., and D. R. Helinski.** 1983. Isolation and characterization of the *recA* gene of *Rhizobium meliloti*. J. Bacteriol. **155:**311–316.
5. **Blount, Z. D., C. Z. Borland, and R. E. Lenski.** 2008. Historical contingency and the evolution of a key innovation in an experimental population of *Escherichia coli*. Proc. Natl. Acad. Sci. U. S. A. **105:**7899–7906.
6. **Boyer, H. W., and D. Roulland-Dussoix.** 1969. A complementation analysis of the restriction and modification of DNA in *Escherichia coli*. J. Mol. Biol. **41:**459–472.
7. **Burmann, B. M., K. Schweimer, X. Luo, M. C. Wahl, B. L. Stitt, M. E. Gottesman, and P. Rösch.** 2010. A NusE:NusG complex links transcription and translation. Science **328:**501–504.
8. **Cannarozzi, G., N. N. Schraudolph, M. Faty, P. von Rohr, M. T. Friberg, A. C. Roth, P. Gonnet, G. Gonnet, and Y. Barral.** 2010. A role for codon order in translation dynamics. Cell **141:**355–367.
9. **Carvalho, F. M., R. C. Souza, F. G. Barcellos, M. Hungria, and T. R. Vasconcelos.** 2010. Genomic and evolutionary comparisons of diazotrophic and pathogenic bacteria of the order *Rhizobiales*. BMC Microbiol. **10:**37.
10. **Castillo, A., H. Taboada, A. Mendoza, B. Valderrama, S. Encarnación, and J. Mora.** 2000. Role of GOGAT in carbon and nitrogen partitioning in *Rhizobium etli*. Microbiology **146:**1627–1637.
11. **Chen, L., P. Zhao, L. Wells, C. T. Amemiya, B. G. Condie, and N. R. Manley.** 2010. Mouse and zebrafish Hoxa3 orthologues have nonequivalent in vivo protein function. Proc. Natl. Acad. Sci. U. S. A. **107:**10555–10560.
12. **Chouard, T.** 2010. Revenge of the hopeful monster. Nature **463:**864–867.
13. **Crossman, L. C., S. Castillo-Ramírez, C. McAnnula, L. Lozano, G. S. Vernikos, J. L. Acosta, Z. F. Ghazoui, I. Hernández-González, G. Meakin, A. W. Walker, M. F. Hynes, J. P. Young, J. A. Downie, D. Romero, A. W. Johnston, G. Dávila, J. Parkhill, and V. González.** 2008. A common genomic framework for a diverse assembly of plasmids in the symbiotic nitrogen fixing bacteria. PloS One **3:**e2567.
14. **Cunin, R., N. Glansdorff, A. Piérard, and V. Stalon.** 1986. Biosynthesis and metabolism of arginine in bacteria. Microbiol. Rev. **50:**314–352.
15. **Dereeper, A., V. Guignon, G. Blanc, S. Audic, S. Buffet, F. Chevenet, J.-F. Dufayard, S. Guindon, V. Lefort, M. Lescot, J.-M. Claverie, and O. Gascuel.** 2008. Phylogeny.fr: robust phylogenetic analysis for the non-specialist. Nucleic Acids Res. **36:**W465–469.
16. **Dunn, M. F., G. Araíza, S. Encarnación, M. C. Vargas, and J. Mora.** 2002. Effect of *aniA* (carbon flux regulator) and *phaC* (poly-β-hydroxybutyrate synthase) mutations on pyruvate metabolism in *Rhizobium etli*. J. Bacteriol. **184:**2296–2299.
17. **Edgar, R. C.** 2004. MUSCLE: multiple sequence alignment with high accuracy and high throughput. Nucleic Acids Res. **32:**1792–1797.

18. **Edger, P. P., and J. C. Pires.** 2009. Gene and genome duplications: the impact of dosage-sensitivity on the fate of nuclear genes. Chrom. Res. **17:** 699–717.
19. **Encarnación, S., M. Dunn, K. Willms, and J. Mora.** 1995. Fermentative and aerobic metabolism in *Rhizobium etli*. J. Bacteriol. **177:**3058–3066.
20. **Encarnación, S., Y. Guzmán, M. F. Dunn, M. Hernández, M. D. C. Vargas, and J. Mora.** 2003. Proteome analysis of aerobic and fermentative metabolism in *Rhizobium etli* CE3. Proteomics **3:**1077–1085.
21. **Encarnación, S., M. Hernández, G. Martínez-Batallar, S. Contreras, M. D. C. Vargas, and J. Mora.** 2005. Comparative proteomics using 2-D gel electrophoresis and mass spectrometry as tools to dissect stimulons and regulons in bacteria with sequenced or partially sequenced genomes. Biol. Proc. Online **7:**117–135.
22. **Encarnación, S., M. C. Vargas, M. F. Dunn, A. Dávalos, G. Mendoza, Y. Mora, and J. Mora.** 2002. AniA regulates reserve polymer accumulation and global protein expression in *Rhizobium etli*. J. Bacteriol. **184:**2287–2295.
23. **Ferraioli, S., R. Taté, E. Caputo, A. Lamberti, A. Riccio, and E. J. Patriarca.** 2001. The *Rhizobium etli argC* gene is essential for arginine biosynthesis and nodulation of *Phaseolus vulgaris*. Mol. Plant-Microbe Interact. **14:**250–254.
24. **Figueroa, N., and L. Bossi.** 1988. Transcription induces gyration of the DNA template in *Escherichia coli*. Proc. Natl. Acad. Sci. U. S. A. **85:**9416–9420.
25. **Figurski, D. H., and D. R. Helinski.** 1979. Replication of an origin-containing derivative of plasmid RK2 dependent on a plasmid function provided in *trans*. Proc. Natl. Acad. Sci. U. S. A. **76:**1648–1652.
26. **Fraser, C., W. P. Hanage, and B. G. Spratt.** 2007. Recombination and the nature of bacterial speciation. Science **315:**476–480.
27. **Fredrick, K., and M. Ibba.** 2010. How the sequence of a gene can tune its translation. Cell **141:**227–229.
28. **Girard, L., S. Brom, A. Dávalos, O. López, M. Soberón, and D. Romero.** 2000. Differential regulation of *fixN*-reiterated genes in *Rhizobium etli* by a novel *fixL-fixK* cascade. Mol. Plant-Microbe Interact. **13:**1283–1292.
29. **González, V., R. I. Santamaría, P. Bustos, I. Hernández-González, A. Medrano-Soto, G. Moreno-Hagelsieb, S. C. Janga, M. A. Ramírez, V. Jiménez-Jacinto, J. Collado-Vides, and G. Dávila.** 2006. The partitioned *Rhizobium etli* genome: genetic and metabolic redundancy in seven interacting replicons. Proc. Natl. Acad. Sci. U. S. A. **103:**3834–3839.
30. **Goryanin, I. I., G. V. Lebedeva, E. A. Mogilevskaya, E. A. Metelkin, and O. V. Demin.** 2006. Cellular kinetic modeling of the microbial metabolism. Methods Biochem. Anal. **49:**437–488.
31. **Guerra, H.** 2007. The brucellae and their success as pathogens. Crit. Rev. Microbiol. **33:**325–331.
32. **Guerrero, G., H. Peralta, A. Aguilar, R. Diaz, M. A. Villalobos, A. Medrano-Soto, and J. Mora.** 2005. Evolutionary, structural and functional relationships revealed by comparative analysis of syntenic genes in Rhizobiales. BMC Evol. Biol. **5:**55.
33. **Guindon, S., and O. Gascuel.** 2003. A simple, fast and accurate algorithm to estimate large phylogenies by maximum likelihood. Syst. Biol. **52:**696–704.
34. **Hanahan, D., J. Jessee, and F. R. Bloom.** 1991. Plasmid transformation of *Escherichia coli* and other bacteria. Methods Enzymol. **204:**63–113.
35. **Hurkman, W. J., and C. K. Tanaka.** 1986. Solubilization of plant membrane proteins for analysis by two-dimensional gel electrophoresis. Plant Physiol. **81:**802–806.
36. **Hynes, M. F., and N. F. McGregor.** 1990. Two plasmids other than the nodulation plasmid are necessary for formation of nitrogen-fixing nodules by *Rhizobium leguminosarum*. Mol. Microbiol. **4:**567–574.
37. **Igarashi, K., and K. Kashiwagi.** 2000. Polyamines: mysterious modulators of cellular functions. Biochem. Biophys. Res. Commun. **271:**559–564.
38. **Kaneko, T., Y. Nakamura, S. Sato, E. Asamizu, T. Kato, S. Sasamoto, A. Watanabe, K. Idesawa, A. Ishikawa, K. Kawashima, T. Kimura, Y. Kishida, C. Kiyokawa, M. Kohara, M. Matsumoto, A. Matsuno, Y. Mochizuki, S. Nakayama, N. Nakazaki, S. Shimpo, M. Sugimoto, C. Takeuchi, M. Yamada, and S. Tabata.** 2000. Complete genome structure of the nitrogen-fixing symbiotic bacterium *Mesorhizobium loti*. DNA Res. **7:**331–338.
39. **Khersonsky, O., and D. S. Tawfik.** 2010. Enzyme promiscuity: a mechanistic and evolutionary perspective. Annu. Rev. Biochem. **79:**11.1–11.35.
40. **Knight, C. G., R. Kassen, H. Hebestreit, and P. B. Rainey.** 2004. Global analysis of predicted proteomes: functional adaptation of physical properties. Proc. Natl. Acad. Sci. U. S. A. **101:**8390–8395.
41. **Korbel, J. O., L. J. Jensen, C. von Mering, and P. Bork.** 2004. Analysis of genomic context: prediction of functional associations from conserved bidirectionally transcribed gene pairs. Nat. Biotechnol. **22:**911–917.
42. **Kovach, M. E., P. H. Elzer, D. S. Hill, G. T. Robertson, M. A. Farris, R. M. Roop II, and K. M. Peterson.** 1995. Four new derivatives of the broad-host-range cloning vector pBBR1MCS, carrying different antibiotic-resistance cassettes. Gene **166:**175–176.
43. **Kudla, G., A. W. Murray, D. Tollervey, and J. B. Plotkin.** 2009. Coding-sequence determinants of gene expression in *Escherichia coli*. Science **324:** 255–258.
44. **Lawrence, J. G.** 2002. Gene transfer in bacteria: speciation without species? Theoret. Pop. Biol. **61:**449–460.
45. **Lemoine, F., O. Lespinet, and B. Labedan.** 2007. Assessing the evolutionary rate of positional orthologous genes in prokaryotes using synteny data. BMC Evol. Biol. **7:**237.
46. **Lind, P. A., C. Tobin, O. G. Berg, C. G. Kurland, and D. I. Andersson.** 2010. Compensatory gene amplification restores fitness after inter-species gene replacements. Mol. Microbiol. **75:**1078–1089.
47. **Livak, K. J., and T. D. Schmittgen.** 2001. Analysis of relative gene expression data using real-time quantitative PCR and the $2^{-\Delta\Delta CT}$ method. Methods **25:**402–408.
48. **Llácer, J. L., I. Fita, and V. Rubio.** 2008. Arginine and nitrogen storage. Curr. Opin. Struct. Biol. **18:**673–681.
49. **Lu, C. D., Z. Yang, and W. Li.** 2004. Transcriptome analysis of the ArgR regulon in *Pseudomonas aeruginosa*. J. Bacteriol. **186:**3855–3861.
50. **Masson-Boivin, C., E. Giraud, X. Perret, and J. Batut.** 2009. Establishing nitrogen-fixing symbiosis with legumes: how many rhizobium recipes? Trends Microbiol. **7:**458–466.
51. **Meade, H. M., S. R. Long, G. B. Ruvkun, S. E. Brown, and F. M. Ausubel.** 1982. Physical and genetic characterization of symbiotic and auxotrophic mutants of *Rhizobium meliloti* induced by transposon Tn*5* mutagenesis. J. Bacteriol. **149:**114–122.
52. **Moreno-Hagelsieb, G., and J. Collado-Vides.** 2002. A powerful non-homology method for the prediction of operons in prokaryotes. Bioinformatics **18:**S329–S326.
53. **Noel, K. D., A. Sánchez, L. Fernández, J. Leemans, and M. A. Cevallos.** 1984. *Rhizobium phaseoli* mutants with transposon Tn*5* insertions. J. Bacteriol. **158:**148–155.
54. **Pappas, K. M.** 2008. Cell-cell signaling and the *Agrobacterium tumefaciens* Ti plasmid copy number fluctuations. Plasmid **60:**89–107.
55. **Phair, R. D.** 1997. Development of kinetic models in the nonlinear world of molecular cell biology. Metabolism **46:**1489–1495.
56. **Piette, J., R. Cunin, A. Boyen, D. Charlier, M. Crabeel, F. Van Vliet, N. Glansdorff, C. Squires, and C. L. Squires.** 1982. The regulatory region of the divergent *argECBH* operon in *Escherichia coli* K-12. Nucleic Acids Res. **10:**8031–8048.
57. **Prentki, P., and H. M. Krisch.** 1984. In vitro insertional mutagenesis with a selectionable DNA fragment. Gene **29:**303–313.
58. **Price, M., K. Huang, E. Alm, and A. Arkin.** 2005. A novel method for accurate operon predictions in all sequenced prokaryotes. Nucleic Acids Res. **33:**880–892.
59. **Proshkin, S., R. A. Rahmouni, A. Mironov, and E. Nudler.** 2010. Cooperation between translating ribosomes and RNA polymerase in transcription elongation. Science **328:**504–508.
60. **Quandt, J., and M. F. Hynes.** 1993. Versatile suicide vectors which allow direct selection for gene replacement in Gram-negative bacteria. Gene **127:** 15–21.
61. **Quintero, M. J., A. M. Muro-Pastor, A. Herrero, and E. Flores.** 2000. Arginine catabolism in the cyanobacterium *Synechocystis* sp. Strain PCC 6803 involves the urea cycle and arginase pathway. J. Bacteriol. **182:**1008–1015.
62. **Quinto, C., H. De la Vega, M. Flores, I. Fernández, T. Ballado, G. Soberón, and R. Palacios.** 1982. Reiteration of nitrogen fixation gene sequences in *Rhizobium phaseoli*. Nature **299:**724–726.
63. **Randhawa, G. S., and R. Hassani.** 2002. Role of rhizobial biosynthetic pathways of amino acids, nucleotide bases and vitamins in symbiosis. Indian J. Exp. Bot. **40:**755–764.
64. **Rocha, E. P.** 2004. Order an disorder in bacterial genomes. Curr. Opin. Microbiol. **7:**519–527.
65. **Sallstrom, B., and S. G. E. Andersson.** 2005. Genome reduction in alphaproteobacteria. Curr. Opin. Microbiol. **8:**579–585.
66. **Shevchuk, N. A., A. V. Bryksin, Y. A. Nusinovich, F. C. Cabello, M. Sutherland, and S. Ladisch.** 2004. Construction of long DNA molecules using long PCR-based fusion of several fragments simultaneously. Nucleic Acids Res. **32:**e19.
67. **Svenningsen, S. L., K. C. Tu, and B. L. Bassler.** 2009. Gene dosage compensation calibrates four regulatory RNAs to control *Vibrio cholerae* quorum sensing. EMBO J. **28:**429–439.
68. **Tabor, C. W., and H. Tabor.** 1985. Polyamines in microorganisms. Microbiol. Rev. **49:**81–99.
69. **Tamames, J.** 2001. Evolution of gene order conservation in prokaryotes. Genome Biol. **2:**R0020.
70. **Thompson, J. D., D. G. Higgins, and T. J. Gibson.** 1994. CLUSTAL W: improving the sensitivity of progressive multiple sequence alignment through sequence weighting, position-specific gap penalties and weight matrix choice. Nucleic Acids Res. **22:**4673–4680.
71. **Tuller, T., A. Carmi, K. Vestsigian, S. Navon, Y. Dorfan, J. Zaborske, T. Pan, O. Dahan, I. Furman, and Y. Pilpel.** 2010. An evolutionary conserved mechanism for controlling the efficiency of protein translation. Cell **141:**344–354.
72. **Zhao, J., D. Ridgway, G. Broderick, A. Kovalenko, and M. Ellison.** 2008. Extraction of elementary rate constants from global network analysis of *Escherichia coli* central metabolism. BMC Syst. Biol. **2:**41.